Effect of Ammonia on the Stability of Colloidal Silver Nanoparticles

by

Waqar Azeem

Supervised by

Dr. Faheem Amin

School Of Natural Sciences,

National University of Sciences and Technology,

H-12, Islamabad, Pakistan.

This Dissertation is dedicated to my parents

for their endless love, support and encouragement.

Acknowledgements

All glory to Almighty Allah, the most merciful and the benevolent and His beloved Prophet Hazrat Muhammad (P.B.U.H).

First of all I would like to express my sincere gratitude to my supervisor Dr. Faheem Amin for his support, patience and priceless guidance in my M.phil research.

I would also like to thank my co-supervisor Dr. Iftikhar Hussain Gul for his guidance and support throughout my research. A special thanks to my guidance and evaluation committee (GEC) members Prof. Dr. Asghari Maqsood, Dr. Waqas Khalid and Dr. Zulqurnain Ali for their help and support in improvement of my work.

I am indebted to the principle of my school "Prof. Dr. Azad Akhtar Siddiqui" who allowed me to pursue my research in experimental physics, it wouldn't have been possible without his backing and struggle. I cannot find words to express my gratitude to the head of the physics department "Dr. Ayesha Khaliq", she is very well behaved and pulchritudinous lady. It is my great pleasure to acknowledge the support and help provided by Dr. Rizwan Khalid. I am thanking most warmly to Dr. Qurat-ul-Ain for her generous contribution in making me understand some significant concepts of the present work.

A very special thanks to my friends Muhammad Jawad and Fahad Azad who were always with me to share every thick and thin during this time. I would also like to acknowledge the beautiful moments spent with Mureed Hussain, Wasim Jamshed, Usama Zaheer, Saqib Husaain and Tahir Amin.

Furthermore, my deepest gratitude goes to my beloved parents, my sisters, brothers and my cousin Muhammad Salman for their endless support, love, prayers and encouragement. I am so lucky to have all of them who provided a carefree environment for me, so that I can concentrate on my studies.

Furthermore, I am grateful to all the technical staff specially Mr. Zeeshan and Mr. Imran for their support in laboratories. I would like to extend my acknowledgements to all the faculty members, staff and students of my institute SNS, NUST for their direct or indirect help.

Waqar Azeem

Contents

List of Figures

List of Tables

Abstract

Silver nanoparticles with narrow size distribution has attained a large interest because of their potential applications in the field of biomedical sciences, catalysis and in printed electronics for the construction of highly conductive elements. The stability of metal nanoparticles has always been a challenge for researchers. A new approach was used to stabilize the silver nanoparticles by the addition of ammonia. Colloidal silver nanoparticles were prepared by Turkevich method in which silver salt is reduced using sodium citrate at 90^oC. It has been noticed that the time of the addition of ammonia, during reaction plays a vital role in the stability of silver nanoparticles. UV-visible absorption spectroscopy was used to determine the effect of particle size on plasmon band as a function of reaction time. No shift in plasmon band as a function of reaction time was noticed after the addition of ammonia. The time of addition of ammonia during reaction has been revealed to be a growth moderating parameter of Ag nanoparticles. Bandgap of Ag nanoparticles was also found by using the Tauc and Davis-Mott models. The crystal structure and the average crystallite size of silver nanoparticles was determined by the X-ray diffraction. It disclosed that synthesized nanoparticles have face centered cubic (FCC) crystal structure. Morphology of the silver nanoparticles was explored by the scanning electron microscope. Shape of the silver nanoparticles found to be spherical and average particle size after the addition of ammonia was found to be 10 nm. The presence of ammonia around silver ions was confirmed by fourier transform infrared spectroscopy (FTIR), the strong absorption peak around 3500 cm^{-1} showed the stretching in N-H bond which was due the interaction of ammonia with silver ions.

Chapter 1

Nanomaterials and Nanotechnology

Nanotechnology plays a fundamental role in the leading technologies of this millennium [1]. "Nano-technology mainly consists of the processing of separation, consolidation, and deformation of materials by one atom or one molecule [2]." The concept that implanted the nanotechnology was first introduced in 1959 by a famous physicist Richard Feynman in his lecture "there is plenty of room at the bottom". The term nanotechnology was first used by Norio Taniguchi: A Professor at Tokyo University of Science [2]. The applications of nanostructures and nanomaterials having size in the range of 1-100 nm is the apparent field of nanoscience and technology.

Nanomaterials usually show divergent physical, electrical, optical, mechanical, chemical and biological properties as compared to their bulk counterparts [3]. In the establishment of the new technology and improvement of the existing these nanoscale materials have found to be very useful. The nanotechnology at the present is in pre-competitive stage and its applied use is very limited, still it is getting used in many industries. These nanoscale materials are important in electronics [4], optoelectronics [5], magnetic, biomedical [6], pharmaceutical, cosmetic, energy and catalytic applications [7].

1.1 Classification of Nanomaterials

Depending upon the number of dimensions that lie in the nano regime, nanomaterials can be classified as:

- Zero Dimensional
- One Dimensional
- Two Dimensional
- Three Dimensional

1.1.1 Zero Dimensional

These are the materials wherein all the dimensions are measured within the nanoscale. The most common illustration of zero dimensional materials are nanoparticles. These nanomaterials can:

- Be amorphous or crystalline
- Exhibit various shapes and forms
- Be single crystalline or polycrystalline

1.1.2 One Dimensional Nanomaterials

One dimensional nanomaterials have one dimension outside the nanoscale. This difference in material dimensions leads needle like shaped nanomaterials. One dimensional nanomaterials comprise nanotubes, nanowires and nanorods. One dimensional nanomaterials can be:

- Chemically pure or impure
- Metallic, ceramic and polymeric

1.1.3 Two Dimensional Nanomaterials

These are the materials in which two dimensions are not bound to the nanoscale. So they exhibit plate like shapes. Two dimensional nanomaterials contains nanofilms, nanolayers and nanocoatings. These materials can be:

- Deposited on a substrate
- Integrated in a surrounding matrix material

1.1.4 Three Dimensional Nanomaterials

Three dimensional nanomaterials are also known as bulk materials. These materials are not bound to nanoscale in any dimension, instead they can have all other nanostructures embedded inside and therefore, it is difficult to classify them. These materials are thus described by having three arbitrary dimensions above 100nm. These materials comprise dispersion of nanoparticles, bundles of nanowires and nanotubes. These materials can be:

- Composite materials
- Composed of multinanolayers

1.2 Properties of Nanoparticles

Nanoparticles have larger surface to volume ratio than their bulk counterparts. So they create a strong effect on surrounding environment as their surface activity increases comparatively. Nanoparticles are being explored for various biotechnological, pharmacological and pure technological uses. They are a link between bulk materials and atomic or molecular structures. Bulk materials have uniform physical properties regardless of their size, whereas in nanoparticles, size does have a significant affect on physical and chemical properties. Thus the properties of the materials change as their size

approaches to the nanoscale and the percentage of atoms on the surface of the materials become more significant.

Nanoparticles are matchless because of their large surface area and this rules the contributions made by the small bulk of the material. Size dependent properties are observed such as quantum confinement in semiconductor particles, surface plasmon in some metal particles and superparamagnetism in magnetic particles.

Nanoparticles exhibit a number of special properties relative to bulk materials. For example bending of bulk copper occurs with movement of copper atoms at about 50 nm scale. But copper nanoparticles do not exhibit the same malleability and ductility as bulk copper because copper nanoparticles smaller than 50 nm are considered as super hard materials. The change in properties is not always desireable, such as ferroelectric materials smaller than 10 nm in all dimensions, can switch their magnetization direction using room temperature thermal energy. This thing make them useless for memory storage. Nanoparticles are small enough to confine their electrons and to produce quantum effects, due to which they exhibit unexpected optical properties. For example, gold nano particles shows transition in their color from deep red to black, with varying size.

1.2.1 Electrical Properties

Electrical properties of nanoparticles are related to the electrical conductivity or conversely to electrical resistivity. Filling factor (ratio of the view areas to the object visible areas) of the connected and empty spaces plays an important role for the electrical conductance of agglomerated nanoparticles or nanosized thin films. For the individually separated nanoparticles, the filling factor is low. The mechanism of conductivity in thin films can be defined by a simple tunnelling between the localized insulating states [8,9] that imply a high resistivity at low temperatures. When the filling factor is large enough for the particles to aggregate into clusters, then a connected path is estab-

lished for the conduction of current. The resistivity ρ will depend on the particle size R, the filling factor f and the aggregation factor A represent the extent to which the particles are attached with each other relative to discrete particles.

The dielectric constant, is the response function of the external field to the local electrical field is closely related to the electrical conductivity and optical properties of the material. The response of dipole displacement in terms of electrons and ions in an external electrical field is described by the dielectric constant. When the metal film thickness and particle size become smaller or similar to the mean free path of the carriers inside the metal, the classical size effect [10], dominates and it affects the dielectric constant.

The quantum size effect arises with further decrease in particle size below the Bohr radius [11]. The conductivity of metallic nanoparticles decreases with the decrease in particle size and below a critical size and temperature these particles behave as non-conducting [12].

1.2.2 Optical properties

To study the optical properties of nanoparticles, different measuring instruments and theories have been utilized. The optical properties of nanoparticles depend on the shape, size, doping and the surrounding medium [13]. The scattering effect on nanoparticles with different shape and sizes was investigated by M. D. Lechner [14]. He used Beer-Lambert law to explain that an extinction coefficient is to calculate the outgoing light intensity from a material. The relation between extinction coefficient and extinction cross section is defined as

$$\ln\left(\frac{I_p}{I}\right) = \tau = \varepsilon c = Nc \tag{1.2.1}$$

Where I_p and I are the intensities of incident and excited light beam respectively. Natural logarithm of these two factors is equal to transmittance, τ is the turbidity coefficient, ϵ is the extinction coefficient c is the particle

concentration and N is the number of particles.

Colour of an object comes from the response of light in eye to the spectra of light absorbed, transmitted or reflected by the object. Colours of suspended nanoparticles, which arise due to the interaction of incident light with the particles, are different from the bulk materials. The main mechanisms that impart the colour to nanoparticle suspensions are: Surface plasmon resonance for metallic nanoparticles and quantum confinement for semiconductor nanoparticles [15].

1.3 Metal Nanoparticles

Metal nanoparticles are very important because of their size and shape dependent properties. The optical properties of these nanoparticles have promoted a great deal of excitement for the last few decades. Infact, there are many examples to find the use of metal nanoparticles as decorative pigments since the Roman times, Laycurgus cup is one of them. The cup can still be seen at the British museum and possesses the unique feature of changing colour depending on light in which it viewed.

The remarkable effect of nanoparticles on color has been known since ancient times when ultra small metal particles were used to color glass in church windows. Silver particles blemished the glass yellow while gold and copper particles were used to make ruby glass [17]. However the nature of these colloids remained unclear until the Faraday explained how metal particles affect the color of church widows [18]. He demonstrated the preparation of gold colloid by reducing an aqueous solution of gold chloride with phosphorus. Nowadays, several other procedures exist for the preparation of noble metal colloids.

1.4 Nanobiotechnology

Nanotechnology and Biotechnology are the most promising technologies of the 21st century. Generally nanotechnology deals with materials, devices and other structures in the nanoscale range and biotechnology deals metabolic and other physiological processes in biological subjects. The combination of these two named as nanobiotechnology, plays a very important role in the study of life. Currently, nanobiotechnology is focused on the attainment of functional nanostructured concepts by the utilization of biological systems such as: cells, cellular components, nucleic acids and proteins, combined with organic and inorganic materials [19].

Nowadays, metal nanoparticles are heavily used in biomedical sciences and engineering. Metal nanoparticles can be synthesized and functionalized with various functional groups like antibodies, ligands and drugs of interest. They find a variety of applications in biotechnology, magnetic separation, targeted drug delivery, vehicles for genes and more importantly in diagnostic imaging. Various imaging techniques like MRI, PET, CT, ultrasound, SERS and optical imaging are used as an aid to image various stages of disease. Difference in techniques and instrumentation of these imaging modalities requires a contrast agent, with unique physiochemical properties. This led to the invention of various nanoparticulated contrast agents for example magnetic nanoparticles, silver and gold nanoparticles for their applications in these imaging modalities.

Chapter 2

Noble Metal Nanopaticles

Nobel metal nanoparticles play an importanat role in the fields of catalysis, biosensing, electronics and optics. Their structure lies in between of molecules and of bulk material, therefore they reduce the gap between molecular chemistry and surface science. Their optical properties are of great interest and these properties mainly depend on a strong absorption in the visible spectrum called the plasmon band, that is the property of colloidal solutions of gold, silver or copper.

2.1 Size of Metal Nanoparticles

In the recent few years metal nanoparticles prepared by solution method have their sizes in micrometer to nanometer range, and microscopic techniques are used to check their morphology and geometric structures. Properties of metal nanoparticles are different from the bulk materials made from the same atoms.

2.1.1 Structural Magic Numbers

Metals comprise 70% of the existing elements. Most metals in the solid state forms are face-centered cubic. This close packed structure have 12 nearest neighbours for each atom. Figure 2.1a shows an FCC lattice in which

single atom is surrounded by 12 atoms and another way of having 12 nearest neighbours is shown in Figure 2.1b, and these 13 atoms make the smallest theoretical nanoparticle for an FCC lattice.

Figure 2.1c shows 14-sided polyhydron which is called a cuboctahedron, generated by connecting the atoms with plannar faces. The three open circles at the upper right of figure 2.1c form the top layer of three atoms of figure 2.1b, the six hard circles and an atom (not pictured) in the center of the cube of figure 2.1c costitute the middle layer of figure 2.1b, and the open circle at the lower left of figure 2.1c is one of the three atoms at the bottom of the cluster of figure 2.1b. This 14-sided polyhydron has six square faces and eight equilateral triangle faces. If another layer of 42 atoms is layed down around the 13 atom nanoparticle, we obtain a 55 atom nanoparticle with the same cuboctahedron shape as shown in figure 2.1d.

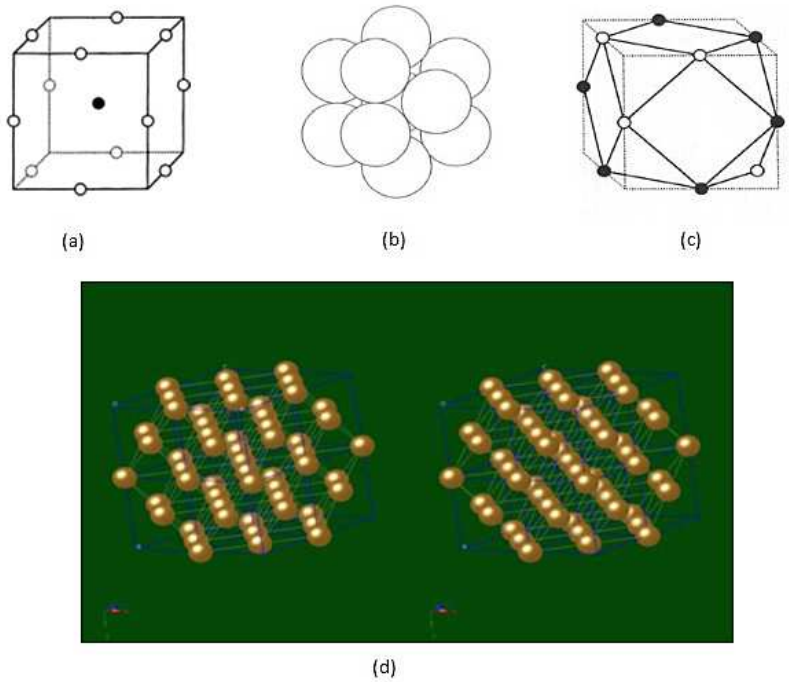

Figure 2.1: a) FCC unit cell, b) a closed packed structure Au_{13} cluster, c) cuboctahedron geometry of Au_{13} [20], d) cuboctahedron geometry of Au_{55}

As the particle becomes smaller the proportion of surface atoms increases. In bulk materials surface atoms form a negligible fraction of the total number of atoms. For FCC metal nanoparticles, the number of atoms on the surface and diameter of each particle is given in table 2.1. The total number of atoms (1, 13, 55, 147,. . .) in particles is called "*structural magic numbers*" [20, 21]. In this FCC nanoparticle for n layers, the number of atoms N is given by the formula:

$$N = \frac{1}{3}(10n^3 - 15n^2 + 11n - 3) \tag{2.1.1}$$

And the number of atoms on the surface is

$$N_{surf} = (10n^2 - 20n + 12) \tag{2.1.2}$$

For diameter of each particle we use the expression $(2n-1)d$ where $\mathbf{d} = \frac{\alpha}{\sqrt{\mathbf{2}}}$ is the distance of nearest neighbour atoms, and α is the lattice constant.

Table 2.1: The relationship between the diameter (d) of the gold nanoparticle, the total number of atoms and the percentage of atoms [20]

Shell	Number of diameters	d, Au nm	Total atoms	Surface atoms	% Surface atoms
1	1d	0.288	1	1	100
2	3d	0.864	13	12	92.3
3	5d	1.44	55	42	76.4
4	7d	2.01	147	92	62.6
5	9d	2.59	309	162	52.4
6	11d	3.16	561	252	44.9
7	13d	3.74	923	362	39.2
8	15d	4.32	1415	492	34.8
9	17d	4.89	2057	642	31.2
10	19d	5.47	2869	812	28.3
25	49d	14.1	4.9×10^4	5083	23.8
50	99d	28.5	4.04×10^5	2.40×10^4	5.9
100	100d	57.3	3.28×10^6	9.80×10^4	3

From table it is clear that the fraction of surface atoms increases with decreasing particle size. A particle of 1 nm would have 76% of the total

atoms on the surface while a nanoparticle of 3 nm with 45% of the total atoms on surface. When particles become smaller than a critical size their properties such as reactivity and melting temperature have been observed to change. The melting point of gold cluster is same as the clusters of gold with more than 100 atoms. The melting point decreases as number of atoms decreases with the size of gold particles. For example, small metal particles with large proportion of surface atoms are highly reactive.

2.2 Optical Properties of Metal Nanoparticles

There are only two coloured metals, copper and gold. All other metals appear silvery because of total reflection of light. For all finely divided metals, the total absorption of light by the large surface makes them dark brown to black. The effect of nanoparticles on color has been known since antique. Plasmon absorbance gives rise to the distinctive colors of colloidal gold, silver and copper. The absorption of electromagnetic radiation on the surface of nanoparticles is due to the collective oscillations in conduction electrons by the incident light.

2.2.1 Surface Plasmons

There are many metals (i.e. alkali metals and noble metals) which can be treated as free electron systems. A metal which contain equal number of fixed positive ions and highly mobile free conduction electrons is called a plasma. The irradiation of electromagnetic wave drives the free electrons by the electric field to oscillate coherently at a plasma frequency of ω_p relative to positive ions [22]. These collective oscillations of free electrons are called plasmons. An electromagnetic wave has a certain penetration depth on a metal surface called skin depth, it is < 50 nm in case of silver and gold, so only the surface electrons are significant for their collective oscillations

which are termed as surface plasmons. And under resonance conditions, the interaction of these plasmons with visible light is called surface plasmons resonance (SPR) [23, 24].

As an example figure 2.2 shows the interaction between light and electrons of metal particle. Surface plasmons resonance happens only when the size of the particle is much smaller than the wavelength of the incident light. The electric field of incident light displace the delocalize electrons in one direction away from the rest of the particle and induce an electric dipole. This produces a net negative charge on one side and positive charge on the opposite side.

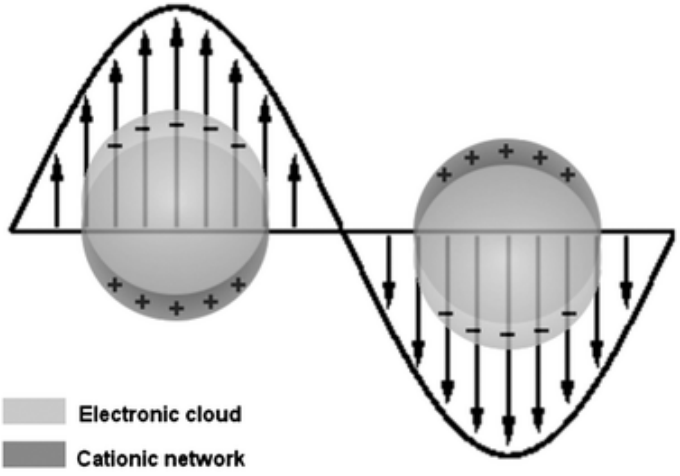

Figure 2.2: Schematic illustration of collective oscillation of free electrons under the effect of an electromagnetic wave [22]

2.2.2 Calculation of Plasmon Band

Surface plasmon band and the factors that determine its position, intensity and broadness are described by the Mie theory and Drude model [25, 26]. Mie theory explains the interaction of light with spherical metal particles. This theory calculates what fraction of light will be absorbed or scattered by the colloidal metal particles. Surface plasmon band or plasmon absorbance

is defined as sum of absorption and scattering of light. The extinction cross section C_{ext} is given by the expression:

$$C_{ext} = \frac{24\pi^2 R^3 \varepsilon_m^{3/2}}{\lambda} \times \frac{\varepsilon''}{(\varepsilon' + 2\varepsilon_m)^2 + \varepsilon''^2} \tag{2.2.1}$$

In this equation R and ε is the particle radius and dielectric constant of the medium respectively. The dielectric function for free electrons in terms of frequency ω is described by the Drude model:

$$\varepsilon' = \varepsilon^{\infty} - \frac{\omega_p^2}{(\omega^2 + \omega_d^2)} \tag{2.2.2}$$

and

$$\varepsilon'' = \frac{(\omega_p^2 \omega_d)}{\omega(\omega^2 + \omega_d^2)} \tag{2.2.3}$$

For a bulk material the bulk plasmon frequency is given by:

$$\omega_p = \sqrt{\left(\frac{Ne^2}{\varepsilon_o m_e}\right)} \tag{2.2.4}$$

Where N is the number density of electrons, ε_o is the dielectric constant of vacuum, m_e and e are the effective mass and charge of an electron respectively. The value of number density for gold is $5.90 \times 10^{28} m^{-3}$ and the calculated value of the surface plasmon resonance for gold is 9.0 eV. The damping frequency ω_d is inversely proportional to the particle size, it increases when the particle size decreases.

The intensity as well as bandwidth and position of surface plasmon absorbance depend on particle size. The dependence of position and band width on particle size is indirectly through the dielectric constant ε, which include the size dependent damping frequency ω_d. As the particle size decreases, the damping frequency increases. The plasmon band broadens with the increase in damping frequency.

2.3 Experimental Results for Plasmon Band

The size, shape and monodispersity of nanoparticles strongly effect the position, shape and intensity of surface plasmon band. Also the interaction

between stabilizing ligands and nanoparticles and the composition of surrounding media may also effect the properties of surface plasmon band [27].

2.3.1 Size of Particles

The experimental results of surface plasmon band for colloidal gold with different diameters are shown in figure 2.3. From the figure, it can be seen that with the increase in particle size there is a decrease in plasmon band frequency. The extinction of light for small gold particles with diameter < 20 nm is primarily due to the absorption of light, but the larger particles exhibit the much stronger scattering [29].

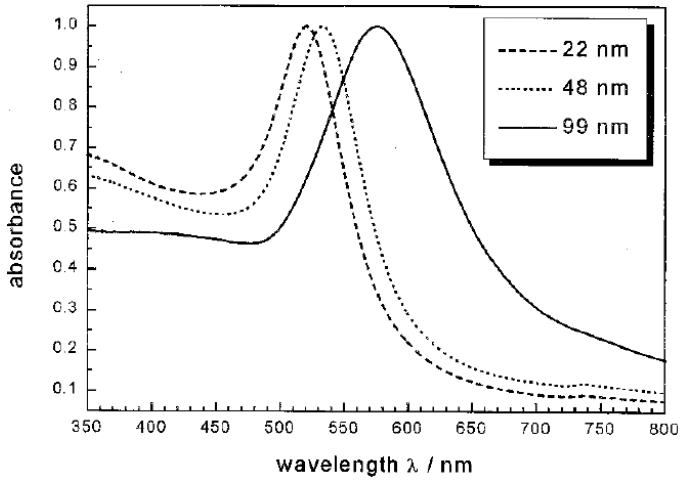

Figure 2.3: Plasmon band for spherical Au particles with different diameters. [29]

2.3.2 Shape of Particles

Plasmon frequencies and plasmon absorbance are strongly affected by the agglomerates of colloidal metal particles. Aggregation of these metal particles lowers their plasmon frequencies and shifts the plasmon band to the longer wavelength [23]. Silver nanoparticles with size 10-14 nm have characteristic absorbance near 400 nm whereas aggregation of silver particles shift the

absorbance peak near 525 nm which decrease the intensity of the plasmon absorbance [33].

2.3.3 Medium Surrounding the Metal Particles

Medium surrounding the metal particles also influence their optical properties. Dielectric environment and surrounding substrate effect the surface plasmon resonance of the metal nanoparticles. The effect of silica slabs on metal nanoparticles varies with the slab dimensions. In case of silver nanoparticles, the presence of silica substrate shifts the extinction peak by about 100 nm to the red [34]. The refractive index of the surrounding medium can also influence the frequency of the surface plasmon band [24]. Normally, a higher refractive index of the medium produces a lower plasmon frequency.

2.4 Preparation of Noble Metal Nanoparticles

The surprising effects of metallic nanoparticles in life sciences have encouraged the development of new techniques for the manufacturing of nanoparticles with required properties. There are variety of physical and chemical methods that can be used to prepare the nanoparticles. Physical and chemical characteristics of the final product determine the choice of the procedure for preparation. The developed techniques for the preparation of metal nanoparticles include chemical reduction using a reducing agent [35], electrochemical reduction [37], photochemical reduction [38], and heat evaporation [39].

In a physical method, a high energy laser is used to evaporate the atoms from the surface of a metal and then these atoms are cooled to nanoparticles. Chemical ways for the preparation of metal nanoparticles are easy to adopt than physical ways, because physical ways usually require a very high temperature, vacuum and expensive equipment and on the other side chemical

methods only use dilute aqueous solutions and cheap equipment.

2.4.1 Reducing Agents

Generally reducing agents are used in chemical reduction reactions in which they react with metal salts to give the metal nanoparticles according to the following equation:

$$mMe^{n+} + nRed \rightarrow mMe^{o} + nOx \tag{2.4.1}$$

The most commonly used reagents with suitable conditions in the reduction of gold, silver and copper salts are listed in table 4.1.

Table 2.2: Procedures for the choice of reducing agents and reaction conditions in the production of gold, silver and copper nanoparticles [40]

Metal Species	E^o/V	Reducing Agent	Conditions	Rate
Au^{3+}	$\geq +0.7$	Alchohol, Polyols	$\geq 70^oC$	Slow
Ag^+		Aldehydes, Sugar	$< 50^oC$	Moderate
		Hydrazine, H_3PO_2	Ambient	Fast
		$NaBH_4$, Boranes	Ambient	Very Fast
		Citrate	$> 70^oC$	Moderate
Cu^{2+}	< 0.7 and ≥ 0	Polyols	$> 120^oC$	Slow
		Aldehydes, Sugar	$70 - 100^oC$	Slow
		Hydrazine, Hydrogen	$< 70^oC$	Moderate
		$AnBH_4$	Ambient	Fast

2.4.2 Synthesis of Nanoparticles

Silver nanoparticles are prepared by the reduction of silver salts [43]. Mostly silver nitrate is used as a starting material. Synthesis of silver nanoparticles by reduction methods may differ in choice of reducing agents, temperature, mixing rate and time of reaction. The size and colour of the silver nanoparticles depends on the reaction conditions. Silver nanoparticles with greenish yellow color and size ranges from 40-60 nm are obtained by the reduction

with sodium citrate at a boiling temperature. Silver nanoparticles of 10 nm size, obtained by reduction with ice-cold sodium borohydrate followed by boiling for one hour showed brownish or yellow green color and absorption maxima at 400 nm (wavelength). [44].

Synthesis of silver nanoparticles with both sodium citrate and sodium borohydride at boiling gives greenish color nanoparticles with particle size 60-80 nm and maximum absorption at the wavelength of 438 nm [45]. Reaction time with sodium borohydrate determines color of the Ag nanoparticles, to be greenish yellow or clear yellow [46].

2.5 Mechanism of Particle Formation

Chemical reduction of metal salts in a solution produce insoluble metal atoms which through slow aggregation leads to the clusters called embryos.

$$xMe^o \leftrightarrow (Me^o_x)_{em} \tag{2.5.1}$$

If the number of atoms which form the metal clusters corresponds to magic numbers then these metal clusters are more stable. A nuclei is formed and separates from the solution as a solid particle, when new metal atoms are introduced into the system which make the embryos to reach a critical size.

$$(Me^o_x)_{em} + yMe^o \rightarrow (Me^o_{X+Y})_{nucl} \tag{2.5.2}$$

With further addition of metal atoms, nuclei grows to nanoparticles size.

$$(Me^o_n)_{nucl} + xMe^o \rightarrow (Me^o_{n+m})_{pp} \tag{2.5.3}$$

After this, either diffusion of atoms on primary particles or aggregation of primary size nanoparticles may results in the formation of final metal particles. These two mechanisms are given by the following equations:

$$(Me^o)_{pp} + nMe^o \rightarrow (Me^o)_p \tag{2.5.4}$$

$$m(Me^o)_{pp} \rightarrow (Me^o)_p \tag{2.5.5}$$

It is quite often that in the same system growth and aggregation mechanisms occur simultaneously. From these two the dominant mechanism determines the shape density of the final particles [40]. High density regular shape metal crystals are supported by the growth mechanism which produce the spherical and lower density metal particles. Gold nanoparticles prepared by aggregation mechanism are shown in figure 2.4.

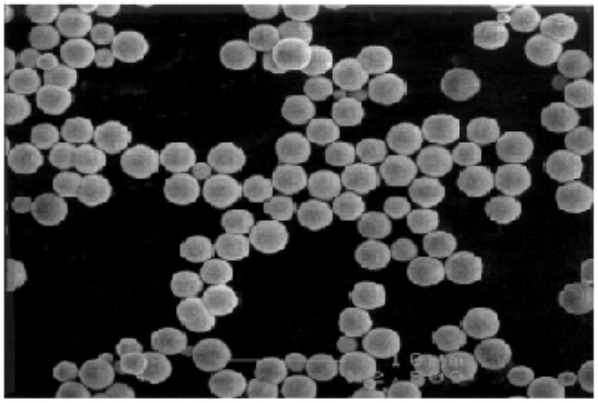

Figure 2.4: SEM of gold nanoparticles obtained by reduction of $HAuCl_4$ with escorbic acid [40]

Supersaturation, degree of aggregation and the fraction of metal atoms to the total amount of metal in the system, determine the final size of the particles [40]. High supersaturation of metal atoms in the system prevents the aggregation mechanism and this will increase the particle size. Slow reactions and slow addition of metal species into the system will create a small number of nuclei and this will produce larger particles.

2.6 Applications of Metal Nanoparticles

The absorption of light by gold and silver nanoparticles is 5-6 order in magnitude of organic dyes. This shows that metal nanoparticles absorb light near infrared and convert it into thermal energy. Therefore, these nanoparticles

can be used in thermal therapy and optical imaging of tumors [54]. High extinction coefficient of silver and gold nanoparticles makes them important as high colorimetric sensors. Optical detection from these sensors can be made by the sensitivity of plasmon peaks to the environmental changes. Silver and gold nanoparticles are used as surface enhanced Raman spectroscopy because of their ability to enhance the local electric fields [55].

Since ancient Greece times silver nanoparticles have been well known for antibacterial activity. Silver nanoparticles have their applications in medicine to reduce infections in burn cure and to avoid bacteria settlement in stainless steel and dental materials.

Chapter 3

Experimental Setup and Measurements

3.1 Fabrication Techniques

Fabrication techniques can be subdivided into two main groups: Top-down techniques, and Bottom up techniques.

3.1.1 Top down approach

In this case materials are derived from a bulk substrate and obtained by gradual removal of material, until the desired nanomaterial is obtained. A simple way to explain the top down method is to think of etching a statue out of a large block of marble.

Several top-down fabricational techniques used in nanotechnologies are derived from semiconductor industry to fabricate the various elements of computers chips. These methods are collectively called lithography in which a light or electron beam is used to selectively remove the micron scale structures from precursor material (resist).

3.1.2 Bottom up approach

Bottom up approach is opposite to the top down approach. In this method we start from the atomic or molecular precursors and obtain the desired

structure by gradually assembling it. Bottom up methods can further divided into two methods:

- Gas phase
- liquid phase

Gas phase methods include plasma arcing and chemical vapour deposition. Liquid phase methods include sol-gel synthesis, which is the most established method whereas, molecular assembly is emerging as a new method.

3.2 Fabrication of Metal Nanoparticles

Fabrication of metal nanoparticles is very easy as compared to ceramic nanoparticles, but it is comparatively difficult to stabilize the metal nanoparticles. Base metal nanoparticles are easily oxidized because of their large surface area. To control this effect surface protecting agents are used, which may sometimes disturb the nanocharacter, when surface effect is used. Generally metal nanoparticles are fabricated by the breakdown or build up methods which are shown in figure 3.1.

In breakdown method a bulk material is crushed by mechanical grinding or mechanical milling. This technique is easy, but it becomes difficult to control the diameter of the particles at the nanolevel, using this technique. The buildup technique has a lot of variations, which are used for assembling metallic atoms. It is further divided into chemical and physical processing.

3.2.1 Chemical Processing

Chemical processing involves the reduction of ions by reducing agents and heating. In metal nanoparticles formation, supersaturation control is important. Mild reducing agents provide ease to control the size of particles in

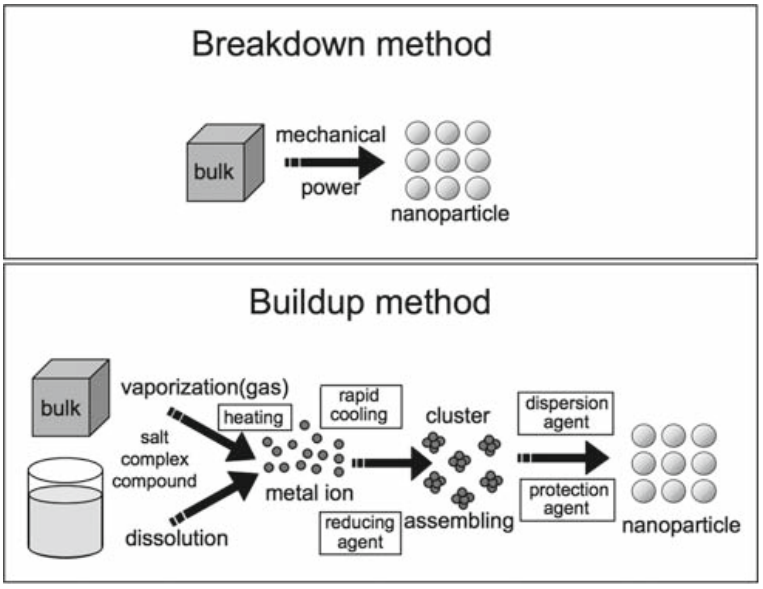

Figure 3.1: Fabricational steps involves in breakdown and build up methods [56]

the nanoparticle fabrication, as it reduces the reduction speed. Hydrazine is strong reducing agent, its use produces large sized particles, and also it becomes difficult to control the size of nanoparticles at fast reaction rate. Organic acids and amine related compounds are not only used as reducing agents, but also as stabilizing agents.

3.2.2 Physical Processing

Opposite to chemical processing, physical processing involves physical power and phase reaction. The example of physical processing is a breakdown method. Phase reactions are further divided into liquid and gas phase methods as shown in figure 3.2 [57].

Among physical processes, gas condensation is the most popular nanoparticle fabrication method. In this method a metallic or inorganic material is vaporized by thermal evaporation sources like inert gas. In gas condensation particle size depends on the time for which the particles remains in the

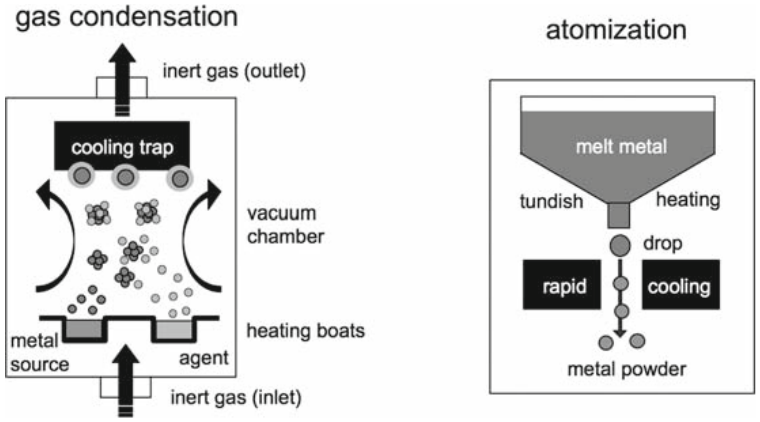

Figure 3.2: Block diagram of gas condensation and atomization.

growth regime and can be affected by the evaporation rate, gas pressure and the kind of inert gas. The other technique is atomization method in which molten metal is quickly cooled into droplets to obtain the metal powder.

3.3 Synthesis of Silver Nanoparticles

Silver nanoparticles are synthesized by the standard method described by the Turkevich [59], in which silver nitrate solution is reduced with tri sodium citrate. As received, analytical grade chemicals were used without further purification in the synthesis of silver nanoparticles. The silver nitrate with 98.8% purity purchased from Sigma Aldrich and Tri-sodium citrate with 99% purity purchased from Sigma Aldrich were used.

To prepare silver nanoparticles 0.1 mmol of silver nitrate were dissolved in 100 ml of deionized water, and then this solution is heated and stirred gently with a magnet teflon coated bar. In another beaker, 0.3 mmol of sodium citrate were dissolved in 1 ml of deionized water and heated it with a magnetic stirring up to 90 ^{o}C. When the silver nitrate solution reached 90 ^{o}C then these solutions were mixed together and after 8-10 min of reaction the mixture became light yellow which was the indication of silver nanoparticles formation.

A second experiment was performed with the same conditions, but immediately after the system became yellow which occurrs after 8 min of reaction, 1 ml (1.4 M) aqueous solution of ammonia was added into the above solution.

3.4 Characterization Techniques

After synthesizing silver nanoparticles in lab, structural characterization was the next goal. In order to characterize the nanoparticles various techniques were used. Based on their principle, these techniques reveal physical, chemical and morphological properties. The brief description of the apparatus and major measurements performed on the sample are:

- UV-Vis Spectroscopy
- X-ray Diffraction (XRD)
- Scanning Electron Microscopy (SEM)
- Fourier Transform Infrared Spectroscopy (FTIR)

3.4.1 UV-Vis Spectroscopy

Ultraviolet visible spectroscopy refers to the absorption and reflectance spectroscopy in the UV-Vis spectral region. The absorption and reflectance in the visible range directly reflects the apparent color of the chemicals involved. UV-Vis spectroscopy is complementary to fluorescence spectroscopy, absorption measure the transition from ground state to higher state, while fluorescence measure the transition from excited state to ground state.

In absorption principle of UV-Vis spectroscopy, molecules containing unbonded electrons can absorb ultraviolet or visible light energy and and get promoted to higher anti-bonding orbitals. If the energy gap between the higher occupied molecular orbital and the lowest unoccupied molecular orbitals is small than the longer wavelength of light can be absorbed. UV-Vis

spectroscopy is mostly used for quantitative determination of different analytes for example transition metal ions. Coloured solutions of transition metal ions are due the excitation of d-electrons from one electronic state to another. Many species like anions or ligands can affect the colour of the metal ion solution and thus change the wavelength of maximum absorption.

Beer Lambert law

This law is used to determine the concentrations of absorbing species in a solution. It describes that path length and concentration of absorbing species control the absorbance of a solution which is given by the following equation.

$$A = \log_{10}\left(\frac{I_o}{I}\right) = \varepsilon.c.L \tag{3.4.1}$$

Where A is the absorbance in units (a.u.), Io and I are the intensities of incident and transmitted light at a given wavelength respectively. ε is a constant for each species and wavelength known as extinction coefficient, c and L are the concentration of the absorbing species and path length through the sample respectively.

UV-visible spectrophotometer is used in UV-Vis spectroscopy. It is used to measure the intensity of light (I) passing through the sample to the intensity of light (Io) before passing through the sample. The transmittance is defined as the ratio I/Io and is measured as ($\%T$). The relation between absorbance (A) and transmittance (T) is defined is given by the equation

$$A = -\log\left(\frac{\%T}{100\%}\right) \tag{3.4.2}$$

The UV-Vis spectrophotometer can also be configured to measure the reflectance and in this measurement it compares the intensity of reflected light from the reference material (I_o) with the intensity of reflected light from the sample (I). The reflectance is the ratio $\frac{I}{I_o}$ which is expressed as a (%R).

3.4.2 X-Ray Diffraction (XRD)

X-Ray diffraction is used to identify the crystalline phases and structural properties of crystalline materials. The arrangements of atoms at interfaces and in amorphous materials can be studied using XRD. Moreover, X-Ray diffraction is helpful in measuring the thickness of thin films and multi layers. This technique use X-rays, which are produced in a cathode ray tube with the source of electrons, and these electrons are accelerated by a high potential. The interaction of these high energy electrons with the metal target produces the electromagnetic radiations which are termed as X-rays. X-Ray diffraction is the most commonly used technique in the experimental physics for the characterization of crystal structures of powder, bulk and thin films.

Bragg's Law

The arrangement of atoms within a crystal are determined by the X-ray crystallography. A crystal is a regular arrangement of atoms, so being an electromagnetic radiation, X-rays can diffract and interfere through the crystal. W. L. Bragg explained that incident waves get partially reflected from parallel planes of the crystal. When these reflected radiations interfere constructively only then the diffracted beam can be obtained. Figure 3.3 shows that the distance between the two adjacent planes is 'd' and when X-rays fall on these adjacent planes they will get reflected with a path difference of $2d\sin\theta$ and interfere constructively only when

$$2dsin\theta = n\lambda \tag{3.4.3}$$

This is called Bragg's law [60].

The reflected radiations from the material give the information about the crystalline structure of that material. Bragg's law is valid only if the inter-planner spacing is comparable with the wavelength of incident radiations ($\lambda \leq 2d$). There are different methods which can be used to determine

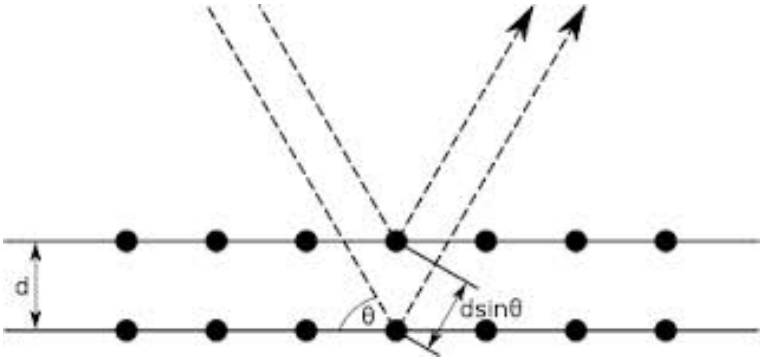

Figure 3.3: Interference between X-ray beams at scattering through crystal planes

the particle size and crystal structure. The most commonly used method for the determination of particle size is the powder method because in this method we use powder of the sample material rather than a single crystal. The information about the diameter of the particle can obtained by the broadening of the peak through the Scherrer's formula given by the following equation

$$t = \frac{0.9\lambda}{\beta cos\theta} \tag{3.4.4}$$

Where t is the diameter of the nanoparticle, β is the full width of the peak at half maximum defined in radians, λ is the wavelength of the incident X-ray beam, and θ is the diffraction angle in degree.

3.4.3 Scanning Electron Microscope (SEM)

When we talk about small scale material characterization the first instrument which would come in our mind is the optical microscope. But for more sophisticated and detailed characterization of a material we use scanning electron microscope. SEM provides a much magnified image of the surface of a material which is similar to that as someone is actually seeing the surface visually. SEM uses a focused beam for the analysis of composition and structure of a sample's surface. This beam of electrons is focused over the surface of a sample through a fine probe. The interaction of electrons with

the surface of the material results in an emission of electrons or photons from the surface.

Appropriate detectors are used to collect the reasonable fraction of the emitted electrons and the output can modulate the brightness of a cathode ray tube. The x-y voltages that rastering the electron beam is synchronised with the x and y input of the cathode ray tube. This will produce an image on the cathode ray tube. Three types of principle images are produced in SEM:

- Secondary Electron Images
- Backscattered Electron Images
- Elemental X-ray maps

Secondary and backscattered electrons, produced by different mechanisms are usually divided according to their energies. Interaction of high energy primary electron with an atom causes an elastic scattering with the atomic nucleus or an inelastic scattering with the atomic electron.

In an inelastic collision nearby electrons gain some amount of energy. If the transfer of energy to the other electrons is very small then the emitted electron will not be able to exit the surface. The emitted electron can only exit from the solid surface if its energy is greater than the work function of the material. If the energy of the emitted electron is less than 50eV then it is called secondary electron. Most secondary electrons are produced near the outer surface of a material but the secondary electrons which are produced deeper inside the material are usually trapped within the material due to inelastic collisions with the other electrons.

High energy primary electrons are scattered from the nucleus of an atom without any loss of kinetic energy. The electrons which exit the specimen with energy more than 50eV are considered as backscattered electros and the energy of these backscattered electrons is comparable to the energy of

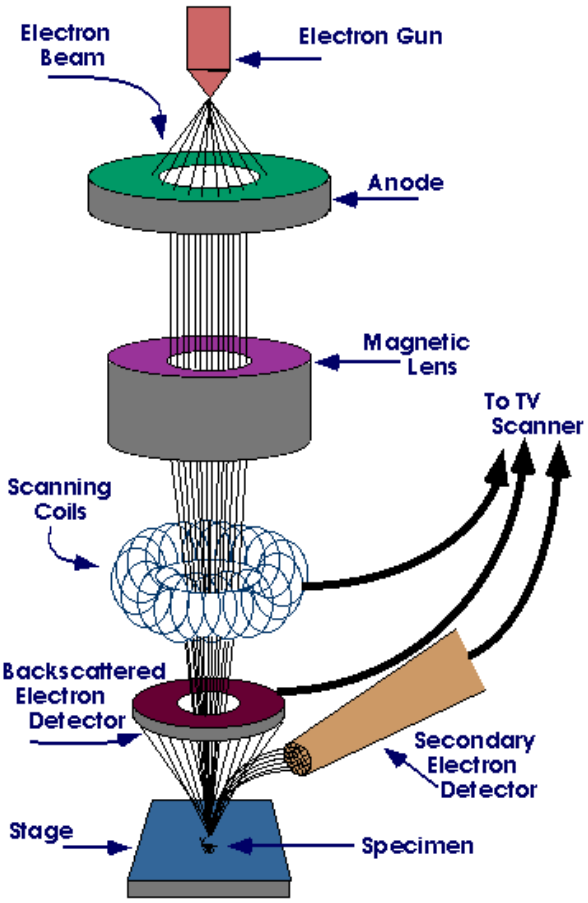

Figure 3.4: Block diagram of Scanning Electron Microscope [61]

primary beam. The backscattering of electrons will occur more likely in a material with higher atomic number (Z). So the brightness of the image will increase when a beam passes from a low Z area to a high Z area.

3.4.4 Fourier Transform Infrared Spectroscopy (FTIR)

FTIR is a technique which is used to identify the nature of the chemical bonds and functional groups in a material. This technique is most commonly used for the non-destructive analysis of thin films and solids. The sensitivity of chemical bonds varies widely in response to different infrared techniques. For example, there is no infrared signal for the carbon-sulphur bond at any

concentration while, there is an infrared signal to detect the silicon-oxygen bond. This shows that infrared spectrophotometry is not applicable as a generic probe but is a function of chemical bond of interest.

The basic infrared experiment is used to determine the changes in the intensity as function of wavelength or frequency of the beam of infrared radiation that interacts with the sample. Infrared spectrophotometer is the central part of this equipment. Infrared spectrophotometer disperses the light from an infrared source and at each frequency measures its intensity. The infrared spectrum is a plot of ratio (of intensity before and after the light interact with the sample) versus frequency.

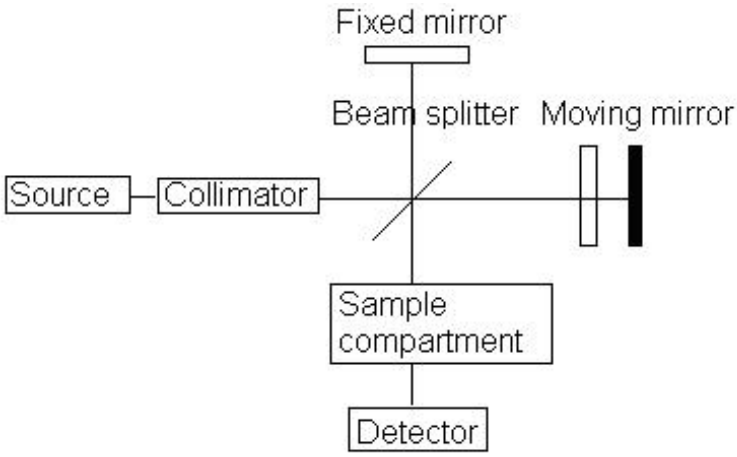

Figure 3.5: Block diagram of FTIR spectrophotometer

Spectrophotometer use Michelson interferometer as a dispersing element. Light generated by a light source falls on a sample after passing through the interferometer. Beam splitter split the light in two directions which are perpendicular to each other. One beam from the splitter strikes the moveable mirror and the other with a fixed mirror and after reflecting these beams again gather at the beam splitter. Constructive and destructive interference takes place at the beam splitter because of change in wave length due to moveable mirror. The recombined beam at the beam splitter falls on the sample and the sample absorb the wavelength of certain characteristic. And

then the intensity time output is recorded by the detector. The Fourier transform convert this energy time out put into intensity versus frequency spectrum.

Chapter 4

Results and Discussions

4.1 Introduction

Silver nanoparticles prepared by different techniques vary in size. The most frequently used method is the reduction method for the preparation of silver nanoparticles. From this method particles with wide range of sizes can be prepared.

Stable colloids of silver nanoparticles have wide range of practical applications in the field of surface-enhanced Raman spectroscopy, catalysis and biosensing in which silver nanoparticles are used as a antibacterial agent. In all these applications silver nanoparticles play an important role. Silver nanoparticles can be prevented from aggregation and precipitation by using different chemicals such as surfactants, mercaptants etc.

Silver nanoparticles prepared by Turkevich method [59], show resemblance with those prepared by Green synthesis that involves minimum waste generation and non toxic substances. In this method silver salt is reduced by mixing it with citrate salt to obtain the silver nanoparticles. The characteristic plasmon band at about 425 nm in visible spectrum indicate the formation of silver nanopartices.

Different variables like temperature and ratios of silver to citrate salts strongly affect the particle size. Synthesis of stabilised silver nanoparticles

with narrow size distribution is always considered to be a challenge in the areas of modern science and technology. In the present wok, a substantial way of preventing the particles from aggregation by the use of ammonia has been described. Ammonia is added in silver/citrate salt solution after the nucleation step to trap all the free Ag^{+} and thus preventing the particle growth and aggregation of new nuclei.

4.2 Effect of Particle Size on Plasmon Band

In metal nanoparticles like silver, conduction and valence bands are very close to each other. The motion of free electrons in valence and conduction band gives rise to the surface plasmon resonance absorption band, which occur due to the resonance of the incident wave with the collective oscillation of electrons of the silver nanoparticles. Spherical silver nanoparticles having size < 20 nm cause a single surface plasmon band.

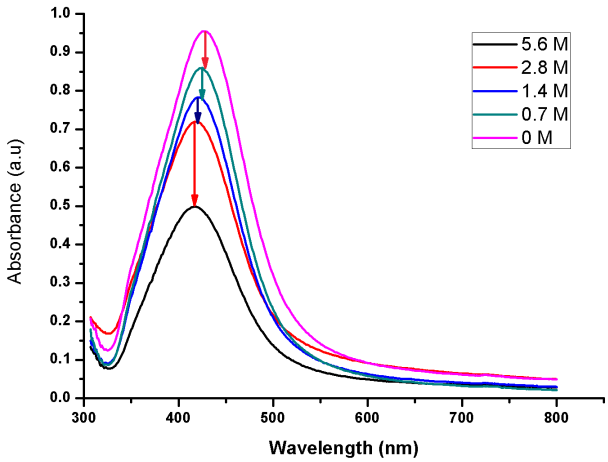

Figure 4.1: Plasmon band for different concentrations of ammonia

UV-visible spectroscopy is an important technique to determine the particle size and optical properties of the nanoparticles. Figure 4.1 shows how different concentration of ammonia affect the plasmon band of Ag nanoparticles. Blue shift in plasmon band indicates the decrease in particle size

with the increase in concentration of ammonia. Surface plasmon band of the silver nanoparticles depends upon the shape, size, free electron density and surrounding medium of the nanoparticles. Due to which UV-Vis spectroscopy is an important tool for monitoring the aggregation of nanoparticles.

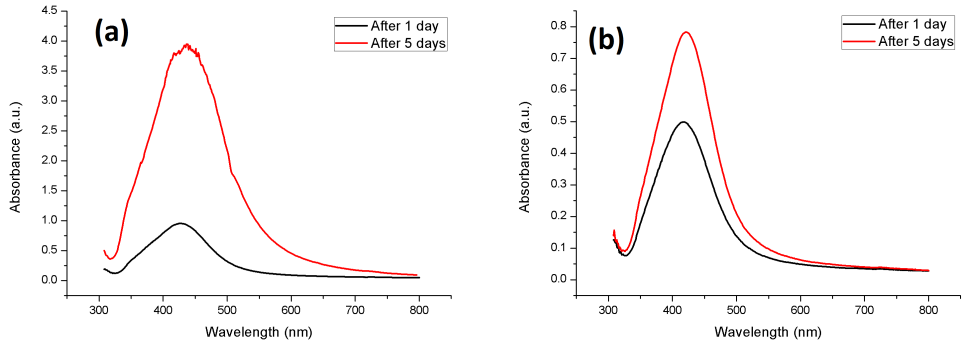

Figure 4.2: UV-visible spectra of colloidal silver nanoparticles (a)with 0 M ammonia (b)with 5.6 M ammonia

For further characterization two samples of Ag nanoparticles was selected one with 0 M ammonia and the other with 5.6 M ammonia shown in Figure 4.2. In figure 4.2a the broadness of surface plasmon band as a function of reaction time shows the increase in particle size, which is in accordance with the quantum size theories [64]. And the increased integrated peak area of the band shows that there is a decrease in interparticle spacing which proves the aggregation of silver nanoparticles.

Figure 4.2b shows the absorption spectra of silver nanoparticles after the addition of ammonia. This shows that there is no change in extinction peak of plasmon band with maturing time. It confirms that the reaction is saturated and the reduction of silver ions to silver atoms is completed at this stage. The positive surface charge on particles surfaces makes the nanoparticles suspensions stable for long time and prevents them from aggregation.

This is due to a strong coulombic repulsion which leads to the metastable solution of single particles [65]. The large clusters will be formed when the

van der waals forces become dominant over coulombic repulsion beyond this metastable state. A decrease in the broadening of extinction peak around 418 nm is due to the addition of ammonia after the nucleation step. Because addition of ammonia trap all the free Ag^{+} and thus prevents the formation of larger particles which cause the intensity of plasmon band to change very slowly, almost no shift in maximum position such as figure 4.3. It also shows fact that there is no further increase in particle size, although there is an increase in nanoparticles concentration.

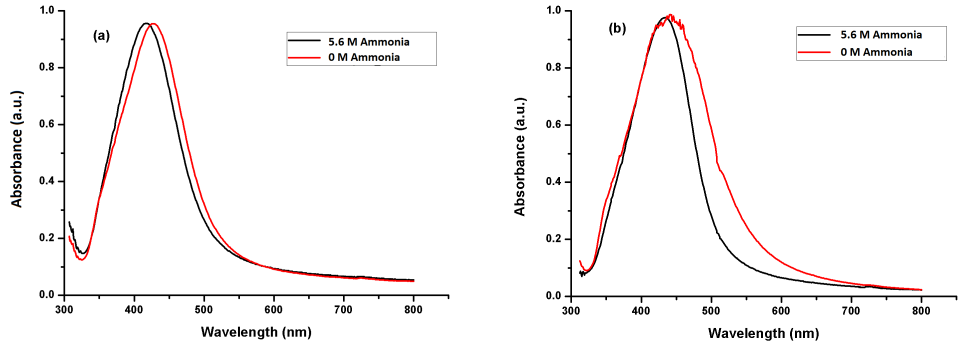

Figure 4.3: Shift in plasmon band for silver nanoparticles (a) after 1 day (b) after 5 days

Figure 4.3a shows the shift of plasmon band towards the lower wave number which indicates the formation of larger particles. This shift in plasmon band points to the fact that particles are still continued to grow as a function of reaction time. But in Figure 4.3b the addition of ammonia in the colloidal suspension of silver nanoparticles shows that there is no shift in maximum position of the plasmon band. This shows that there is no increase in particle size however the concentration of particles increased slightly with time.

Band gap of Ag NPs

The optical band gap of Ag nanoparticles was calculated by using the absorption spectra. The absorption coefficient and nature of interband tran-

sition is calculated by using the following relation [66].

$$\alpha = \frac{1}{d \ln(\frac{1}{T})} \tag{4.2.1}$$

$$(\alpha h\nu)^n = A(h\nu - E_g) \tag{4.2.2}$$

in equation 4.2.1 d is the path length (width of the cuvette) and T is the transmittance, which is related to the absorption by the following relation

$$A = \log[\frac{1}{T}] \tag{4.2.3}$$

In equation 4.2.2 E_g is the band gap energy, A is a constant and n denotes the type of transition. For direct band gap n=2 and for indirect band gap $n = 1/2$. As in case of pure metals only direct band transitions are allowed. The value of the direct band gap for Ag NPs after 1 day of reaction time was calculated by extrapolating the linear part of the curve at $\alpha = 0$ and it is found to be 3.55 eV for 0 M ammonia and 3.6 eV for 5.6 M ammonia shown in figure 4.4. This shows that Ag NPs with small size have large band gap, so they can behave as semiconductors.

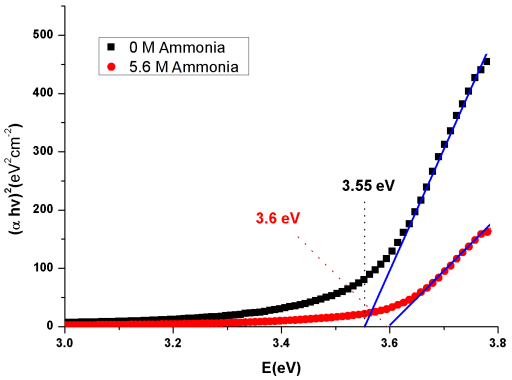

Figure 4.4: Band gap of Ag NPs after 1 day of reaction time

After 5 days of reaction time the band gap of Ag NPs with ammonia was found to be same as after 1 day, but there is a negligible band gap for Ag NPs with 0 M ammonia indicated the increase in particle size. This decrease

in band gap also indicating the metallic behaviour of Ag NPs shown in figure 4.5.

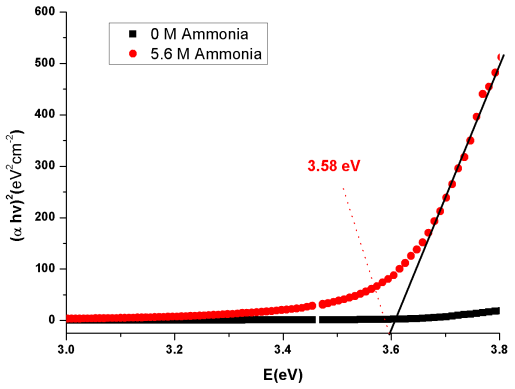

Figure 4.5: Band gap of Ag NPs after 5 days of reaction time

4.3 XRD Analysis of Silver Nanoparticles

In XRD CuK_α X-rays of wavelength $\lambda = 1.5406A^o$ was used for the analysis of the prepared sample of the silver nanoparticles. The sample was prepared by spreading the aqueous colloidal solution of silver nanoparticles on the glass substrate, it was then dried at 40^o to evaporate the solvent. Sample was taken, than scanned keeping in 2θ ranges from 20^o to 90^o. In first step indexing of the diffraction pattern is done and the Miller indices to each plane were assigned. Strong Bragg reflections corresponds to the planes (111), (200), (220) and (311) as shown in figure. The diffraction patterns confirms the structure of the synthesized silver to be face centered cubic (FCC).

No peaks of impurities were found in the diffraction pattern. This thing indicate that all peaks refer to pure silver metal with FCC structure. The crystallinity degree of the silver nanoparticles is reflected from the high intense peak at (111) reflections. Noise in the diffraction pattern is probably

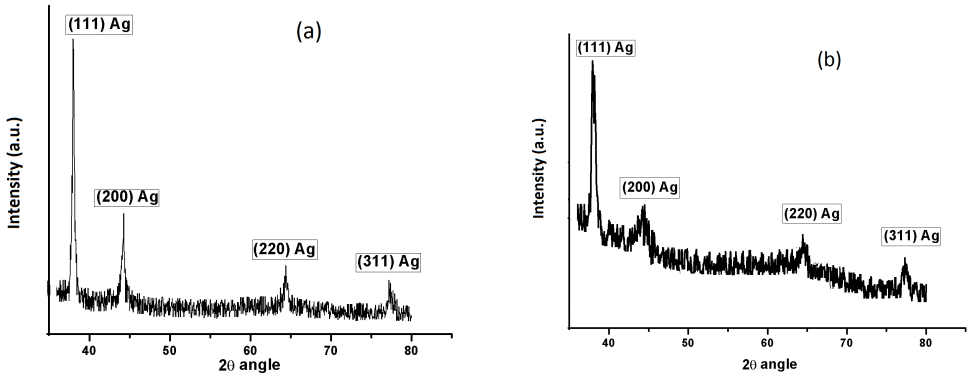

Figure 4.6: XRD pattern showing 2θ positions and indices of the silver nanoparticles synthesized at 90^o using glass substrate as a sample holder (a)with 0 M ammonia (b)with 5.6 M ammonia

due to the glass substrate on which the particles were scanned. As, the purpose of this work was to increase the stability of Ag NPs. So, the powder of Ag NPs was difficult to obtain. In order to study the structure of these particles we scanned a dried drop of these particles on glass substrate. The 2θ values 38.119, 44.305, 64.452 and 77.409 degree corresponds to planes (111), (200), (220) and (311) of silver are in agreement with the standard diffraction card of JCPDS, silver file No. 04-0783.

Lattice constant can be measured by using the Bragg's law (equation 3.4.3). For cubic structure the relation between lattice constant and the planar spacing is given by the following equation:

$$a = d_{hkl}\sqrt{h^2 + k^2 + l^2} \tag{4.3.1}$$

where d is the planar spacing and h, k and l are the Miller indices. Combining equations 3.4.3 and 4.3.1 the value of the planar spacing was found which is 2.36 Å. And from equation 4.3.1 the value of the lattice constant found to be 4.0876 Å which is very similar to value of 4.08 Å found on the JCPS card.

Scherrer formula [68] is used to calculate the average crystallite size of

the silver nanoparticles which is given by the following equation:

$$D = \frac{0.9\lambda}{\beta \cos\theta} \tag{4.3.2}$$

Where D is the diameter of the particle, λ is the wavelength of the incident X-Ray and β is the full width at half maximum value in radian. The average value of crystallite size calculated from this equation is 28 nm for the particles without ammonia and 10 nm for the particles with ammonia. The density of the sample was calculated by using the following relation

$$\rho_x = \frac{4M}{N_a a^3} \tag{4.3.3}$$

Where M is the molecular mass of Ag, N_a is the Avogadro's number. Surface area of Ag nanoparticles can also be calculated by using the following equation

$$s = N.(4\pi r^2) \tag{4.3.4}$$

In this equation N denotes the number of atoms in one gram of the material, and can be calculated using this relation.

$$N = \frac{Volume\ of\ 1\ gram}{\frac{4}{3}\pi(1/2\ the\ avg\ crystallite\ size)^3} \tag{4.3.5}$$

The values of density and surface area given in the following table are in agreement with the reported results [69].

Table 4.1: Structural analysis of Ag NPs using XRD

Type of Sample	a ($\mathring{A}$)	ρ (g/cm^3)	s (m^2/g)
without ammonia	4.08	10.5	20.4
with ammonia	4.08	10.5	48

4.4 SEM of Ag Nanoparticles

Synthesis of nanoparticles is a very elusive process, which is affected by different parameters. In nanoparticles synthesis environmental effects and preparation methods determine the shape of synthesized nanoparticles. The change in environmental parameters or the methods of preparation may cause the change in structure and physical properties of the synthesized silver nanoparticles.

Scanning electron microscopy is used to determine the morphology of the silver nanoparticles. SEM graphs of silver nanoparticles (with ammonia and without ammonia) prepared by reduction method are shown in figure 4.7(a) and (b). For SEM analysis of silver nanoparticles a suspension of silver nanoparticles in methanol was made and sonicated for 40 mins. After this a small drop was spread on glass substrate to deposit the silver nanoparticles on it and allowed the methanol to evaporate at room temperature.

A thin layer of gold particles was deposited on the silver nanoparticles to make them conductive for the operation of machine. SEM results show that the shape of prepared silver nanoparticles is spherical. And the silver nanoparticles functionalized with ammonia have average size of 13 nm as shown in figure 4.7(a), which revealed that addition of ammonia clearly affects the stability of silver nanoparticles.

It shows that monodisperse and highly crystalline silver nanoparticles are obtained. And the silver nanoparticles with 0 M ammonia have the average diameter of 33 nm shown in figure 4.7(b).

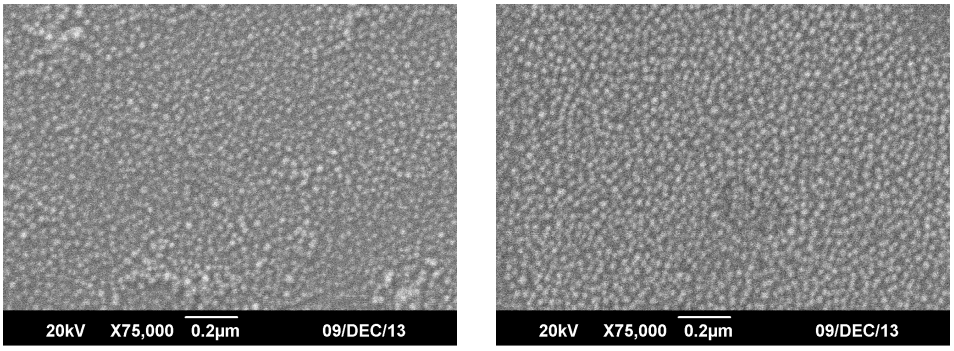

Figure 4.7: SEM results of silver nanoparticles (a) with 5.6 M ammonia (b) with 0 M ammonia

4.5 FTIR Spectroscopy of Silver Nanoparticles

In fourier transform infrared spectroscopy potassium bromide pellet (KBr) was used as a sample holder. KBr pellet was prepared by keeping the KBr powder under pressure of 5 tons for 3 minutes. After this a small drop of silver nanoparticles suspension was spread on KBr pellet. The host salt was selected in such a way that it was irresponsive for region of spectrum in which we were interested, hence no contribution from the Potassium bromide pellet was found in the spectrum. Sometimes it might be possible that KBr contribute in the spectrum due its hygroscopic nature, which can be neglected by taking the background spectrum of KBr pellet. The FTIR spectra of silver nanopaticles is in agreement with the reported results [70].

Figure 4.8(a), shows the FTIR spectra of silver nanoparticles with 0 M ammonia. The strong absorption peak at 1637.73 cm^{-1} and 1384.51 cm^{-1} indicate the presence of NO_2 that is coming from the precursor solution of $AgNO_3$ involved in the synthesis of silver nanoparticles. The absorption peaks around 3400 cm^{-1} represents the O-H stretching mode [71], which

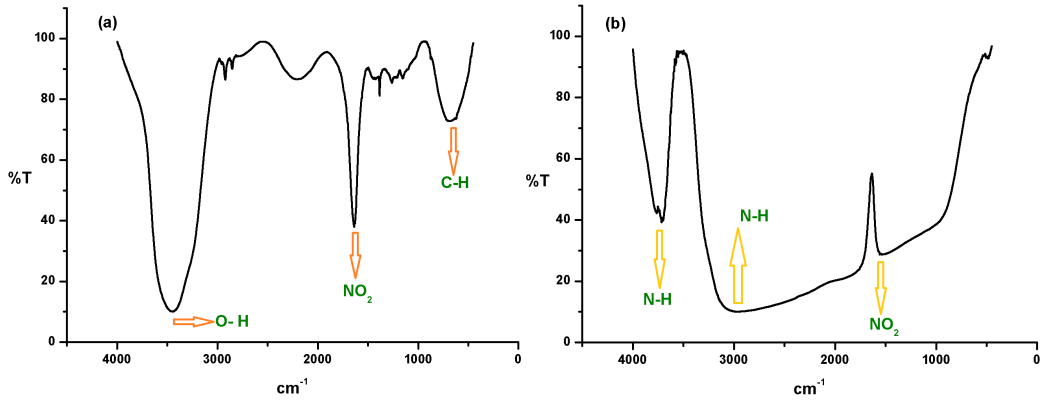

Figure 4.8: FTIR spectra of Ag NPs (a) with 0 M ammonia (b) with 5.6 M ammonia

is due to the interaction of water with the surface of silver nanoparticles whereas the absorption peaks at 1100-1300 cm^{-1} represent the C-O stretching mode. Figure 4.8(b), shows the FTIR spectra of silver nanoparticles after the addition of ammonia. The purpose of addition of ammonia in silver nanoparticles solution after the nucleation step was to trap all free Ag^{+}, and soluble diamine silver (I) complex $[Ag(NH_3)_2]^{+}_{(aq)}$ formed instantly. The very strong absorption peaks at 3763.89 cm^{-1} and 3716.23 cm^{-1} represent the N-H stretching mode, which is due to the interaction of ammonia with the free silver ions. And the absorption peak at 2900 cm^{-1} represents the N-H bending mode. This shows that the addition of ammonia affect the morphology of the silver nanoparticles.

Chapter 5

Conclusion and Future Recommendation

A simple and new method has been introduced for the stability of colloidal silver nanoparticles. The effect of ammonia on the stability of silver nanoparticles was studied in this work firstly by the UV-visible spectroscopy. It was observed that addition of ammonia after the nucleation step in reaction flask trapped all the free silver ions by making soluble diamine silver (I) complex, thus prevented the further reduction of silver ions into silver atoms. UV-visible spectra of two different samples with and without ammonia was taken. The shift in plasmon band was clearly observed as function of reaction time in a sample without ammonia, which confirms the increase in particle size. There was no shift in plasmon band for a sample having ammonia showed that there was no change in particle size with the passage of time, but there was a small increase in concentration of particles. It has also been observed that these particles remain stable for several weeks.

Bandgap of the samples with 0 M and 5.6 M ammonia were estimated and it was concluded that the bandgap of samples with 5.6 M ammonia remains almost constant whereas, a noticeable change in the band gap without ammonia was seen due to increase in particle size. X-ray diffraction of silver nanoparticles confirmed the face centered cubic crystalline structure. The average crystallite size calculated for the most intense peak (111) using

Scherrer formula was found to be 28 nm for 0 M ammonia, and 10 nm for the sample with 5.6 M ammonia. Scanning electron microscope witnessed the spherical shape of silver nanoparticles.

SEM analysis was performed on both samples, and it was observed that particles containing ammonia have narrow size distribution and the average particle size was found to be 12 nm. And for the sample without the addition of ammonia it was found to be 33 nm. The strong absorption peak at 3763.89 cm^{-1} and 3716.23 cm^{-1} in FTIR spectroscopy confirmed the presence of ammonia on silver ions.

The ultrasmall Ag nanoparticles (< 2 nm) show a reasonable band gap. The PL measurements of these clusters is underway. The magnetic properties of the clusters will be studied to explore a further possibility of second transition i.e. from optical to magnetic behavior. Furthermore, the surface of the clusters will be tailored to passivate them for biological applications.

References

[1] D. Mandal, M. E. Bolander, D. Mukhopadhyay, G. Sarkar, P. Mukherjee, Appl. Microbiol. Biotechnol. 69, 485, 2006

[2] N. Taniguchi, "On the Basic Concept of Nano-Technology", Proc. Intl. Conf. Prod. Eng. Tokyo, Part II, Japan Society of Precision Engineering, 1974

[3] V. K. Sharma, R. A.Yngard, Y. Lin, Adv. Colloid Interfac. 145, 83, 2009

[4] http://biologicalfuelcell.wordpress.com/biological-fuel-cells/

[5] J. Shi, Y.Zhu, X. Zhang, Willy R.G. Baeyens, Ana M. Garcaia-Campana, Trends in Analytical Chemistry, 23, 351, 2004

[6] J.S. Kim, A.E. Kuk, B.K.N. Yu, Nanomed. Nanotechnol. Biol. Med. 3, 95, 2007

[7] P. Liu, M. Zhao, Appl. Surf. Sci. 255, 3989, 2009

[8] L. J. Chen, J. H. Tyan, and J. T. Lue, Phys. Chem. Solids 55, 871, 1994

[9] G. Reiss, J. Vancea, and H. Hoffmann, Phys. Rev. Lett. 56, 2100, 1986

[10] X. Sun, Y. N. Xiong, P. Chen, J. Y. Lin, W. Ji, J. H. Lim, S. S. Yang, D. J. Hagan, and E. W. Van Stryland, "Investigation of an optical limiting mechanism in multiwalled carbon nanotubes", Appl. Opt. 39, 12, 2000

[11] W. C. H. a. J. T. Lue, Phys. Rev. B, vol. 49, 1994

[12] A. Chatterjee, D. Chakaravorty, "Electrical conductivity of Sol jel derived metal nanoparticles", J. M. Science, 27, 4115, 1992

[13] X. Z. X. Zhang, W. Shi, X. Meng, C. Lee, Shuittong Lee, J. Phys. Chem, vol. 109, 2005

[14] M. D. Lechner, "Influence of Mie scattering on nanoparticles with different particle sizes and shapes: Photometry and Analytical Ultracentrifugation with Absorption Optics", Search Results Journal of the Serbian Chemical Society, vol. 70, pp. 361-369, 2005

[15] M. A. E.-S. S. Eustis, "Why gold nanoparticles are more precious than pretty gold: noble metal surface plasmon resonance and its enhancement of the radiative and nonradiative properties of nanocrystals of different shapes", Chem. Soc. Rev. vol. 35, pp. 209-217, 2006

[16] Available: www.thebritishmuseum.ac.uk/science/text/lycurgus/sr-lycurgus-p1-t.html

[17] Klabunde, K. Ed. Nanoscale Materials in Chemistry, Wiley Interscience: New York page; 23, 2001

[18] C. P. Poole, and Owens, F. J. Introduction to Nanotechnology. New Jersey: Wiley Interscience, 2003

[19] C. M. M. C. A. Niemeyer, Nanobiotechnology Concepts, applications and perspectives. Weinheim, Germany: Wiley-CH Verlag GmbH and Co. KGaA. 2004

[20] C. P. Poole, and Owens, F. J. Introduction to Nanotechnology. New Jersey: Wiley Interscience, 2003

[21] K. Klabunde, Ed. Nanoscale Materials in Chemistry. New York: Wiley Interscience, 2001

[22] Y. Xia, and Halas, N. J. "Shape-controlled synthesis and surface plasmonic properties of metallic nanostructures", MRS Bulletin, vol. 30, pp. 338-343, 2005

[23] A. Moores, and Goettmann, F. "The plasmon band in noble metal nanoparticles: an introduction to theory and applications", New Journal of Chemistry, vol. 30, pp. 1121-1132, 2006.

[24] P. Mulvaney, "Surface plasmon spectroscopy of nanosized metal particles", Langmuir, vol. 12, pp. 788-800, 1996

[25] G. Mie, "Contributions to the optics of turbid media, particularly of colloidal metal solutions", Annalen der Physik, vol. 25, pp. 377-445, 1908

[26] L. Drude, "On the electron theory of metals", Annalen der Physik 1, vol. 3, pp. 566-613, 1900

[27] I. Lisiecki, and Pileni, M. B. "Synthesis of copper metallic cluster using reverse micelles as microreactors", Journal of American Society, vol. 115, pp. 3887-3896, 1993

[28] L. Lisiecki, Billoudet, F. and Pileni, P., "Control of the shape and the size of copper metallic particles", Journal of Physical Chemistry, pp. 4160-4166, 1996

[29] M. El-Sayed, and Link, S., "Shape and size dependence of radiative, nonradiative and photothermal properties of gold nanocrystals," International Reviews in Physical Chemistry, vol. 19, pp. 409-453, 2000

[30] M. P. Pileni, "Optical properties of nanosized particles dispersed in colloidal solutions or arranged in 2D or 3D superlattices," New Journal of Chemistry, pp. 693-702, 1998

[31] M. P. Pileni, "Nanosized particles made in colloidal assemblies," Langmuir, vol. 13, pp. 3266-3276, 1997

[32] J. Tanori, and Pileni, M. P., "Control of the shape of copper metallic particles by using a colloidal system as template", Langmuir, vol. 13, pp. 639-646, 1997

[33] S. Solomon, Bahadory, M. Jeyarajasingam, A. Rutkowsky, S. Boritz, C. and Mulfinger, L., "Synthesis and study of silver Nanoparticles" Journal of Chemical Education, vol. 84, pp. 322-325, 2007

[34] L. K. Kelly, Coronado, E., Zhao, L., and Schatz, G. C., "The optical properties of metal nanoparticles: the influence of size, shape, and dielectric environment", Journal of Physical Chemistry B, vol. 107, pp. 668-677, 2003

[35] H. Wang, Qiao, X., Chen, J., and Ding, S., "preparation of silver nanoparticles by chemical reduction method," Colloids and Surface A: Physicochemical and Engineering Aspects, vol. 256, pp. 111-115, 2005

[36] S. Panigrah, Kundu, S., Ghosh, S. K., Nath, S., and Pal, T., "General method of synthesis for metal nanoparticles", Journal of Nanoparticle Research, vol. 6, pp. 411-414, 2004

[37] D. Zhang, W., Chen, C., Zhang, J., and Ren, F., "Fabrication of nanosized metallic copper by electrochemical milling process", Journal of Material Science, vol. 43, pp. 1492-1496, 2008

[38] M. H. Maillard, P. and Brus, L., "Silver nanodisck growth by surface plasmon enhanced photoreduction of desorbed [Ag+]", Nano letters, vol. 3, pp. 1611-1615, 2003

[39] C. H. Bae, Nam, S. H., and Park, S. M., "Formation of silver nanoparticles by laser ablation of a silver target in NaCl solution" Applied Surface Science, vol. 628, pp. 197-198, 2002

[40] D. V. Goia, and Matijevic, E., "Preparation of monodispersed metal particles," New Journal of Chemistry, pp. 1203-1215, 1998

[41] J. Wagner, Tshikhudo, T., and Koehler J., "Microfluidic generation of metal nanoparticles by borohydride reduction", Chemical Engineering Journal, vol. 135, pp. S104-S109, 2008

[42] C. Cao, Park, S., and Sim, S., "Seedless synthesis of octahedral gold nanoparticles in condensed surfactant phase", Journal of Colloid and Interface Science, vol. 322, pp. 152-157, 2008

[43] D. R. Van Hyning, Klemperer, W. G., and Zukowski, C. F., "Silver nanoparticle formation: predictions and verification of the aggregative growth model", Langmuir, vol. 17, pp. 3128-3135, 2001

[44] P. C. M. Lee, D., "Adsorption and Surface-Enhanced Raman of dyes on silver and gold sols", Journal of Physical Chemistry, vol. 86, pp. 3391-3395, 1982

[45] A. S. Nair, and Pradeep, T. Y, , "Halocarbon mineralization and catalytic destruction by metal nanoparticles", Current Science, vol. 84, 2003

[46] Y. Fang, "Optical absorption of nanoscale colloidal silver: aggregate band and adsorbate-silver surface band", Journal of Physical Chemistry, vol. 108, pp. 4315-4318, 1998

[47] Z. Nikhil J., L. W., Tapan, K. S., and Tarasankar, P., "Seed-mediated growth method to prepare cubic copper nanoparticles", Current Science, vol. 79, pp. 1367-1370, 2000

[48] S. Kapoor, and Mukherjee, T., "Photochemical formation of copper nanoparticles in PVP", Chemical Physics Letters, vol. 370, pp. 83-87, 2003

[49] S. H. Wu, and Chen, D. H., "Synthesis of high concentration Cu nanoparticles in aqueous CTAB solutions", Journal of Colloid and Interface Science, vol. 273, pp. 165-169, 2004

[50] H. H. Huang, Yan, F. Q., Kek, Y. M., Chew, C. H., Xu, G. Q., Ji, W., and Tang, S. H., "Synthesis, characterization, and nonlinear optical properties of copper nanoparticles", Langmuir, vol. 13, pp. 172-175, 1997

[51] B. K. Park, Jeong, S., Kim, D., Moon, J., Lim, S., and Kim, J. S., "Synthesis and size control of monodisperse copper NPs by polyol method", Journal of Colloid and Interface Science, vol. 311, pp. 417-424, 2007

[52] A. A. Athawale, Prachi P., Kumar, M., and Majumdar, M. B., "Synthesis of CTAB-IPA reduced copper nanoparticles," Materials Chemistry and Physics, vol. 91, pp. 507-512., 2005

[53] Y. Wang, Chen, P., and Liu, M., "Synthesis of well-defined copper nanocubes by a one-pot solution process", Nanotechnology, vol. 17, pp. 6000-6006, 2006

[54] L. R. Hirsch, Stafford, R. J., Bankson, J. B., Sershen, S. R., Rivera, B., Price, R. B., Hazle, D., and Halas, N. J., "Nanoshell-mediated near-infrared thermal therapy of tumors under magnetic resonance guidance", PNAS, vol. 100, pp. 13549-14554, 2003

[55] Hyunhyub Ko, Srikanth Singamaneni, and Vladimir V. Tsukruk, Nanostructured Surfaces and Assemblies as SERS Media, W. Inter Science. vol. 10, 15761599, 2008

[56] H. T. Y. Hayashi M. Inoue, and K. Suganuma, Nanoparticle Fabrication. Portland: Springer, 2008

[57] H. Gleiter "Nanocrystalline materials" Prog. Mater. Sci, vol. 33, pp. 233-315, 1990

[58] C. Granqvist, R. Buhrman "Ultrafine metal particles" J. Appl. Phys, vol. 47, pp. 2200-2207, 1976

[59] P. C. S. J. Turkevich, S. Hiller, Discuss. Faraday Soc., vol. 11, 1951

[60] Charles Kittel, Introduction to Solid State Physics. Newyork: John Wiley and Sons Inc, 1976

[61] http://www.puredue.edu/rem/rs/sem.htm

[62] http://en.wikipedia.org/wiki/Atomic force microscopy

[63] Robert A. Wilson, Heather A. Bullen, "Introduction to Scanning Probe Microscopy", Northern Kentucky University, Highlands

[64] C. J. Addison and A. G. Brolo, Langumir 22, 8696, 2006

[65] M. Meyer, E. C. Ru, and P. G. Etchegoin, J. Phys. Chem. B 110, 6040, 2006

[66] Khan W, Cao C, Yu Ping D, Nabi G, Hussain S, Butt F and Cao T, Mater. Lett. vol. 65 pp. 1264, 2011

[67] Ratnika Varshney, Seema Bhadauria, Mulayam S.Gaur, Adv. Mat.Lett. 1(3), 232, 2010

[68] Rita John, S. Sasi Florence, Chalcogenide Lett.6, 535, 2009

[69] Jo-Yong Park, Yun-Jo Lee, Ki-Won Jun, Jin-Ook Baeg, Dae Jae Yim, J.of Ind. and Eng Chem. 12, 882, 2006

[70] T. Theivasanthi, M. Alagar, "Electrolytic Synthesis and Characterizations of Silver Nanopowder", 2011

[71] K. Nakamoto, Infrared Spectra of Inorganic and Coordination Compounds, Wiley, New York

[72] Navendu Goswami, P. Sen, Solid State Comm. 132, 791, 2004